

## Structure of the Lightest Tin Isotopes

T. D. Morris,<sup>1,2</sup> J. Simonis,<sup>3,4</sup> S. R. Stroberg,<sup>5,6</sup> C. Stumpf,<sup>3</sup> G. Hagen,<sup>2,1</sup> J. D. Holt,<sup>5</sup> G. R. Jansen,<sup>7,2</sup>  
T. Papenbrock,<sup>1,2</sup> R. Roth,<sup>3</sup> and A. Schwenk<sup>3,4,8</sup>

<sup>1</sup>*Department of Physics and Astronomy, University of Tennessee, Knoxville, Tennessee 37996, USA*

<sup>2</sup>*Physics Division, Oak Ridge National Laboratory, Oak Ridge, Tennessee 37831, USA*

<sup>3</sup>*Institut für Kernphysik, TU Darmstadt, Schlossgartenstraße 2, 64289 Darmstadt, Germany*

<sup>4</sup>*ExtreMe Matter Institute EMMI, GSI Helmholtzzentrum für Schwerionenforschung GmbH, 64291 Darmstadt, Germany*

<sup>5</sup>*TRIUMF 4004 Wesbrook Mall, Vancouver, British Columbia V6T 2A3, Canada*

<sup>6</sup>*Physics Department, Reed College, Portland, Oregon 97202, USA*

<sup>7</sup>*National Center for Computational Sciences, Oak Ridge National Laboratory, Oak Ridge, Tennessee 37831, USA*

<sup>8</sup>*Max-Planck-Institut für Kernphysik, Saupfercheckweg 1, 69117 Heidelberg, Germany*

 (Received 21 September 2017; revised manuscript received 12 January 2018; published 12 April 2018)

We link the structure of nuclei around  $^{100}\text{Sn}$ , the heaviest doubly magic nucleus with equal neutron and proton numbers ( $N = Z = 50$ ), to nucleon-nucleon ( $NN$ ) and three-nucleon ( $NNN$ ) forces constrained by data of few-nucleon systems. Our results indicate that  $^{100}\text{Sn}$  is doubly magic, and we predict its quadrupole collectivity. We present precise computations of  $^{101}\text{Sn}$  based on three-particle–two-hole excitations of  $^{100}\text{Sn}$ , and we find that one interaction accurately reproduces the small splitting between the lowest  $J^\pi = 7/2^+$  and  $5/2^+$  states.

DOI: [10.1103/PhysRevLett.120.152503](https://doi.org/10.1103/PhysRevLett.120.152503)

**Introduction.**— $^{100}\text{Sn}$  is a nucleus of superlatives: It is the heaviest self-conjugate ( $N = Z = 50$ ) nucleus [1], exhibits the largest strength in allowed  $\beta$  decay [2], is close to the proton dripline [3], and is the end point of a region of nuclei with enhanced  $\alpha$  decays [4,5]. While these properties make  $^{100}\text{Sn}$  the cornerstone of a most interesting region of the nuclear chart, our understanding of this nucleus and its neighbors is still rather limited; see Ref. [6] for a review. No data exist regarding the spectrum of  $^{100}\text{Sn}$ , and the spin assignments for low-lying states in  $^{101}\text{Sn}$  are controversial [7,8]. Likewise, the evolution of collective observables towards neutron number  $N = 50$  is experimentally unclear at present [9–18]. On the other hand, with naively expected shell closures for both protons and neutrons, and the stabilizing effects of the Coulomb and centrifugal barriers,  $^{100}\text{Sn}$  should be particularly suitable for a reliable theoretical treatment.

In this Letter, we calculate properties of  $^{100}\text{Sn}$  and neighboring nuclei using realistic interactions between protons and neutrons. This is in contrast to large-scale shell-model (LSSM) calculations [19–23] in this region of the nuclear chart that employ  $^{80}\text{Zr}$  or  $^{88}\text{Sr}$  cores and phenomenologically adjusted interactions based on the  $G$ -matrix approach [24]. The strong nuclear force is rooted in the fundamental theory of strong interactions, quantum chromodynamics (QCD), and is manifested in dominant two-nucleon ( $NN$ ) forces and weaker but pivotal three-nucleon ( $NNN$ ) forces between protons and neutrons. Effective field theories (EFTs) of QCD provide us with a systematically improvable low-momentum expansion of

these interactions [25–27]. So far, interactions derived from the EFT framework have been applied to light- and medium-mass nuclei (see Refs. [28–31] for recent reviews).

The extension of *ab initio* computations from lighter [28,29,32] to heavier nuclei is based on the development and application of quantum many-body methods that exhibit a polynomial scaling in mass number [33–43]. Medium-mass and heavy nuclei can technically be computed with these methods, but most interactions developed thus far considerably overbind heavier nuclei [44]. In the quest for nuclear interactions with more acceptable saturation properties [45–48], one interaction labeled 1.8/2.0(EM) has emerged that describes binding energies, two-neutron separation energies, and the first  $2^+$  excited state in nuclei up to neutron-rich nickel isotopes remarkably well, while charge radii are too small [49–54]. It is primarily this interaction from Ref. [45] that we will employ in the computation of  $^{100}\text{Sn}$  and its neighbors.

This Letter is organized as follows. First, we briefly describe the Hamiltonian, the employed model spaces, and computational methods. Then, we validate the interactions in the tin region by computing known binding energies and level splittings, and address method uncertainties by employing the coupled-cluster method [30,55] and the valence-space in-medium similarity-renormalization-group method (VS-IMSRG) [56] coupled with the importance-truncated large-scale shell model [57]. Finally, we present results for the structure of the lightest isotopes of tin.

**Hamiltonian and model space.**—We employ the intrinsic Hamiltonian

$$H = \sum_{i<j} \left( \frac{(\mathbf{p}_i - \mathbf{p}_j)^2}{2mA} + V_{NN}^{(i,j)} \right) + \sum_{i<j<k} V_{NNN}^{(i,j,k)}, \quad (1)$$

where the  $NN$  and  $NNN$  potentials ( $V_{NN}$  and  $V_{NNN}$ , respectively) are the interactions 1.8/2.0(EM), 2.0/2.0(EM), 2.2/2.0(EM), and 2.0/2.0(PWA) from Ref. [45]. These interactions result from a similarity-renormalization-group (SRG) [58] evolution of the chiral  $NN$  interaction of Ref. [59] to cutoffs  $\lambda = 1.8, 2.0$ , and  $2.2 \text{ fm}^{-1}$ . The  $NNN$  potential is not evolved but rather taken as the leading  $NNN$  forces from chiral EFT [60–62] and has a cutoff  $\Lambda_{NNN} = 2.0 \text{ fm}^{-1}$ . The two low-energy constants of the short-range part of the  $NNN$  forces are adjusted to the binding energy of the triton and the radius of the  $\alpha$  particle, following Ref. [63]. This refitting procedure presumably captures the induced short-ranged  $NNN$  forces from the  $NN$  SRG evolution. These interactions are quite soft (due to the relatively small cutoffs), which allows us to achieve reasonably well-converged binding energies and spectra in nuclei up to neutron-rich  $^{78}\text{Ni}$  [51,54], and in the neutron-deficient tin isotopes considered in this work.

Figure 1 shows the computed ground-state energies per nucleon for  $^4\text{He}$ ,  $^{16}\text{O}$ ,  $^{40,48}\text{Ca}$ ,  $^{56}\text{Ni}$ ,  $^{90}\text{Zr}$ , and  $^{100}\text{Sn}$  with the single-reference IMSRG [38,40]. The 1.8/2.0(EM) interaction consistently yields the best agreement with data. Presently, it is unclear what distinguishes this interaction from the other similarly obtained interactions; however, this soft interaction puts us in a fortuitous situation to make theoretical predictions (albeit without rigorous uncertainty quantification) for binding energies and spectra in nuclei as heavy as  $^{100}\text{Sn}$ .

Coupled-cluster calculations use a Hartree-Fock basis constructed from a harmonic-oscillator basis of up to 15 major oscillator shells. For VS-IMSRG we use a similar basis, except that the Hartree-Fock reference is constructed with respect to an ensemble state above the  $^{80}\text{Zr}$  core following Ref. [56]. All calculations are performed at oscillator frequencies in the range  $\hbar\omega = 12\text{--}16 \text{ MeV}$ , which include the minimum in energy for the largest model space we consider. We use the normal-ordered two-body approximation [39,44,64] for the  $NNN$

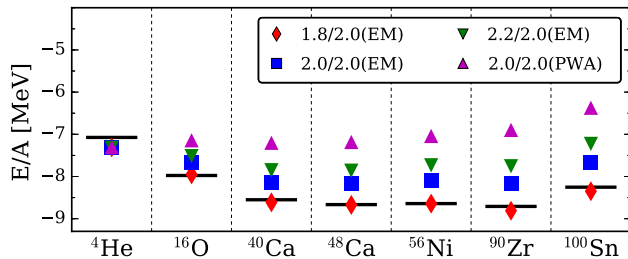


FIG. 1. Ground-state energies per nucleon  $E/A$  for selected closed-shell nuclei computed with the closed-shell IMSRG [38] using the interactions of Ref. [45] in comparison with experiment (black horizontal lines).

interaction with an additional energy cut on three-body matrix elements  $e_1 + e_2 + e_3 \leq E_{3 \text{ max}}$ . Here  $e_i$  are single-particle energies (in units of  $\hbar\omega$ ) of the harmonic-oscillator basis. When  $E_{3 \text{ max}}$  is increased from 16 to 18, the binding energy of  $^{100}\text{Sn}$  changes by 2% for the hardest interaction 2.0/2.0(PWA), while for the softest interaction, 1.8/2.0(EM), the change is less than 1%.

*Method.*—The coupled-cluster method is an ideal tool to compute doubly magic nuclei and their neighbors [30,33,34,36,37,42,65–67]. This method computes the similarity transform  $\bar{H} \equiv \exp(-T)H_N \exp(T)$  of the normal-ordered Hamiltonian  $H_N$ , obtained by normal-ordering the free-space Hamiltonian (1) with respect to the closed-shell Hartree-Fock reference of  $^{100}\text{Sn}$ . The cluster operator  $T$  includes particle-hole excitations and is truncated at the coupled-cluster singles-doubles (CCSD) level. Usually CCSD accounts for about 90% of the correlation energy (i.e., the energy beyond Hartree-Fock) [55]. For a higher precision of the ground-state energy, we include triples excitations of the cluster operator  $T$  perturbatively within the  $\Lambda$ -CCSD(T) method [68]. Excited states in  $^{100}\text{Sn}$  are computed with an equation-of-motion (EOM) method including  $3p$ - $3h$  corrections via a generalization of the ground state  $\Lambda$ -CCSD(T) approximations to excited states with EOM-CCSD(T) [69]. The neighboring nuclei  $^{101,102}\text{Sn}$  are computed as one- and two-particle attached states [70–72] of the  $^{100}\text{Sn}$  similarity-transformed Hamiltonian  $\bar{H}$ . The two-particle attached states of  $^{102}\text{Sn}$  are truncated at the  $3p$ - $1h$  level, while the particle-attached states of  $^{101}\text{Sn}$  are computed at the  $2p$ - $1h$  level with perturbative  $3p$ - $2h$  corrections included (described below). Further details of the coupled-cluster approach to nuclei are presented in a recent review [30].

We briefly describe our new approach to include perturbative  $3p$ - $2h$  corrections to the particle-attached states of  $^{101}\text{Sn}$ . Generalizing the completely renormalized (CR) EOM-CCSD(T) approximation from quantum chemistry [73,74] and nuclear physics [42,66,75] to particle-attached excited states yields the correction

$$\delta\omega_\nu^{3p-2h} = \sum_{i<j} \sum_{a<b<c} \mathcal{L}_{\nu,ij}^{abc} \mathcal{R}_{\nu,ij}^{abc} \mathcal{M}_{\nu,ij}^{abc}. \quad (2)$$

Here  $\nu$  denotes the state of interest;  $i, j$  (and  $a, b, c$ ) are occupied (and unoccupied) orbitals in the  $^{100}\text{Sn}$  reference  $|\Phi\rangle$ ;  $\mathcal{L}_\nu$  and  $\mathcal{M}_\nu$  represent the left and right  $3p$ - $2h$  moments

$$\mathcal{L}_{\nu,ij}^{abc} = \langle \Phi | \mathcal{L}_\nu^{2p-1h} \bar{H} | \Phi_{ij}^{abc} \rangle, \quad \mathcal{M}_{\nu,ij}^{abc} = \langle \Phi_{ij}^{abc} | \bar{H} \mathcal{R}_\nu^{2p-1h} | \Phi \rangle;$$

$|\Phi_{ij}^{abc}\rangle$  are  $3p$ - $2h$  excited states; and  $\mathcal{R}_\nu$  is the resolvent

$$\mathcal{R}_{\nu,ij}^{abc} = \langle \Phi_{ij}^{abc} | (\omega_\nu^{2p-1h} - \bar{H})^{-1} | \Phi_{ij}^{abc} \rangle. \quad (3)$$

Here  $\omega_\nu^{2p-1h}$  is the  $2p$ - $1h$  energy corresponding to the left ( $\mathcal{L}_\nu^{2p-1h}$ ) and right ( $\mathcal{R}_\nu^{2p-1h}$ ) eigenstates of  $^{101}\text{Sn}$ . We draw the reader's attention to the similar structure between the bivariational expression (2) and second-order perturbation

theory. This method is the completely renormalized particle-attached equation of motion (CR-PA-EOM). In our results for  $^{101}\text{Sn}$ , we used three different approximations (labeled *A*, *B*, *C*) for the energy denominator in Eq. (3). Approximation *A* uses in place of  $\bar{H}$  the Hartree-Fock single-particle energies, approximation *B* uses the one-body part of  $\bar{H}$ , and approximation *C* uses both the one- and two-body parts of  $\bar{H}$ . Thus, approximation *C* is the most complete choice for the resolvent and most accurately approximates the full calculation [66].

The IMSRG and its VS-IMSRG variant are effective tools for computing doubly magic nuclei and for constructing valence-space interactions from  $NN$  and  $NNN$  interactions that can be subsequently diagonalized using shell-model techniques [31,38,56,76–78]. These methods also rely on similarity transformations  $\bar{H} \equiv \exp(\Omega)H_N \exp(-\Omega)$ , where  $H_N$  is the normal-ordered Hamiltonian with respect to the ensemble reference of each target nucleus. For nuclei in the  $^{100}\text{Sn}$  region, the VS-IMSRG yields an anti-Hermitian  $\Omega$ , truncated at the one- and two-body level, which decouples the major oscillator shell above  $^{80}\text{Zr}$ . The ensuing large-scale eigenvalue problem is solved via the importance-truncated shell model [57].

*Results.*—Results for  $^{100}\text{Sn}$  are shown in Fig. 2. Figure 2(a) shows the low-lying states in  $^{100}\text{Sn}$  computed in the EOM-CCSD and EOM-CCSD(T) approximations with the 1.8/2.0(EM) interaction. We also show the phenomenological LSSM results of Ref. [2]. The relatively large excitation gap of about 4 MeV is consistent with  $^{100}\text{Sn}$  being doubly

magic, a finding which is—to our knowledge—qualitatively ubiquitous in all previous theoretical investigations. Figure 2(b) shows our EOM-CCSD predictions for the  $B(E2)$  transition in  $^{100}\text{Sn}$  for the 1.8/2.0(EM), 2.0/2.0(EM), 2.2/2.0(EM), and 2.0/2.0(PWA) interactions together with the experimental  $B(E2)$  values for the isotopes  $^{104-132}\text{Sn}$  [9–14]. Our computed  $B(E2)$  values are similar in size to that of  $^{132}\text{Sn}$  and consistent with  $^{100}\text{Sn}$  being doubly magic. They also fall within expectations from phenomenological shell-model calculations [6] and from extrapolations of data in light tin isotopes. For  $^{100}\text{Sn}$ , the computed  $B(E2)$  values are a bit smaller than the LSSM results of Ref. [12]. Figure 2(c) shows EOM-CCSD (for  $^{100}\text{Sn}$ ) and two-particle attached EOM-CC (for  $^{102}\text{Sn}$ ) results for 1.8/2.0(EM), 2.0/2.0(EM), 2.2/2.0(EM), and 2.0/2.0(PWA) interactions and the VS-IMSRG result for the 1.8/2.0(EM) interaction for the energy of the first  $J^\pi = 2_1^+$  state in light even isotopes  $^{100-110}\text{Sn}$ , and data for  $^{102-132}\text{Sn}$ . The  $B(E2)$  values computed are consistent with the computed excitation energies of the first  $J^\pi = 2_1^+$ , in the sense that, for a given interaction, the larger the energy, the smaller the  $B(E2)$  value. We note that despite the consistency with experiment, the 1.8/2.0(EM) interaction produces radii that are too small, and this would certainly affect the  $B(E2)$ . The systematic trend of known and computed  $2_1^+$  energies in the tin isotopes again suggests that  $^{100}\text{Sn}$  is doubly magic. In  $^{100}\text{Sn}$ , this energy is similar to that of the doubly magic nucleus  $^{132}\text{Sn}$  [79,80]. The VS-IMSRG result for the  $2_1^+$  state

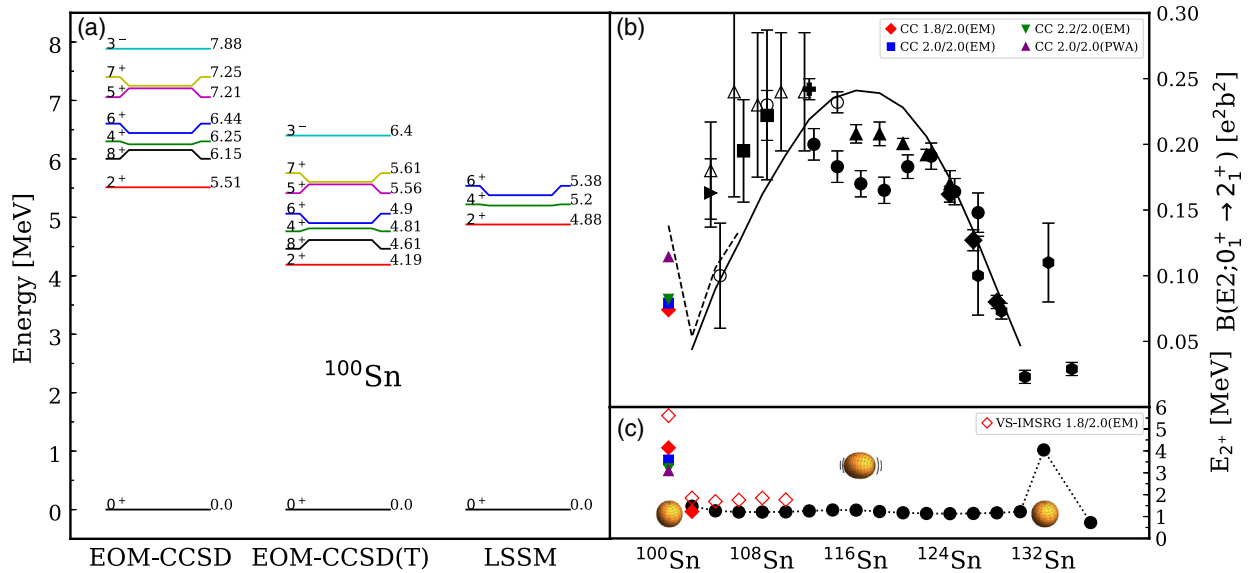


FIG. 2. Panel (a) shows low-lying states in  $^{100}\text{Sn}$  computed with the chiral interaction 1.8/2.0(EM) in the EOM-CCSD and EOM-CCSD(T) approximations and compared to LSSM calculations based on phenomenological interactions [6]. Panel (b) shows the EOM-CCSD results for the  $B(E2)$  transition strength in  $^{100}\text{Sn}$  with the interactions as indicated, and the experimental data for all other even tin isotopes. The full (dashed) line is taken from LSSM as reported in Ref. [6] (Ref. [12]). Panel (c) shows the energy of the  $J^\pi = 2_1^+$  states in even tin isotopes, with coupled-cluster results for  $^{100,102}\text{Sn}$  [labeled as in panel (b)] and VS-IMSRG results for  $^{100-110}\text{Sn}$  with interactions as indicated, and data for  $^{102-132}\text{Sn}$  (black circles). The shapes illustrate the absence or presence of collectivity.

in  $^{100}\text{Sn}$  is about 1.5 MeV higher than the EOM-CCSD(T) result, but close to the similarly approximated EOM-CCSD result shown in Fig. 2(a). Using the discrepancy between methods as an estimate of the uncertainty in the many-body method, our results for the energy of the  $2_1^+$  state in  $^{102-110}\text{Sn}$  are consistent with the data.

In  $^{101}\text{Sn}$ , the two lowest states are separated by only 172 keV [7,8]. Observation of  $^{105}\text{Te}$   $\alpha$  decay in coincidence with the 172 keV  $\gamma$  line indicates that the dominant  $\alpha$  decay of  $^{105}\text{Te}$  is to the first excited state in  $^{101}\text{Sn}$ , implying that these states have identical spins [8]. We recall that the lowest two states in the odd isotopes  $^{105-113}\text{Te}$  and  $^{101-105}\text{Sn}$  are only about 0.2 MeV apart and lack definite spin assignments. In tin, this near degeneracy between the  $J^\pi = 5/2^+$  and  $7/2^+$  states persists up to  $^{111}\text{Sn}$ , and the ground-state spin changes from  $J^\pi = 5/2^+$  in  $^{107}\text{Sn}$  [81] and  $^{109}\text{Sn}$  to  $J^\pi = 7/2^+$  in  $^{111}\text{Sn}$ . The level ordering in  $^{101}\text{Sn}$  to  $^{105}\text{Sn}$  between the  $J^\pi = 5/2^+$  and  $7/2^+$  states is not known. This is reflected in Fig. 3(a), which compares available data (full and open black points for definite and tentative spin assignments, respectively) with particle-attached EOM-CC and VS-IMSRG predictions for the energy splitting in odd tin isotopes using the interactions 1.8/2.0(EM) and 2.0/2.0(EM). Both interactions yield a small splitting between the  $J^\pi = 5/2^+$  and  $7/2^+$  states, but they differ on its precise size and sign. Figure 3(b) plots the calculated energy splitting between the  $J^\pi = 5/2^+$  and

$7/2^+$  states versus the neutron separation energy of  $^{101}\text{Sn}$  computed with the CR-PA-EOM using the 1.8/2.0(EM), 2.0/2.0(EM), 2.2/2.0(EM), and 2.0/2.0(PWA) interactions. Also shown are estimated uncertainties due to finite model-space sizes and the employed methods, and a blue (diagonal) band encompassing these uncertainties (see Ref. [49] for details). The horizontal and vertical green lines indicate experimental data. The intersection of the blue diagonal band with the precisely known neutron separation energy  $S_n$  yields one estimate of the systematic uncertainty for the energy splitting between the  $J^\pi = 5/2^+$  and  $7/2^+$  states in  $^{101}\text{Sn}$ . Clearly, theory is not sufficiently precise to make a definite prediction for the ground-state spin of  $^{101}\text{Sn}$ , as the predicted range for the energy splitting can support either  $J^\pi = 5/2^+$  or  $7/2^+$  as the ground state. Again, the 1.8/2.0(EM) interaction is closest to data. We note that spacings from the different (EM) interactions vary by about 1 MeV. This cutoff dependence suggests that the simple refit of the  $NNN$  contacts does not fully capture the induced forces from the SRG evolution. Figure 3(c) shows the lowest states in  $^{101}\text{Sn}$ , computed with the  $2p$ - $1h$  particle-attached EOM-CC method, the CR-PA-EOM developed in this work, and the VS-IMSRG for the 1.8/2.0(EM) interaction. We find that for this interaction, the different methods agree on the level ordering, and the energy splitting varies by at most 140 keV. While the upcoming measurements will yield definite spin assignments [82], getting theory to a level where such

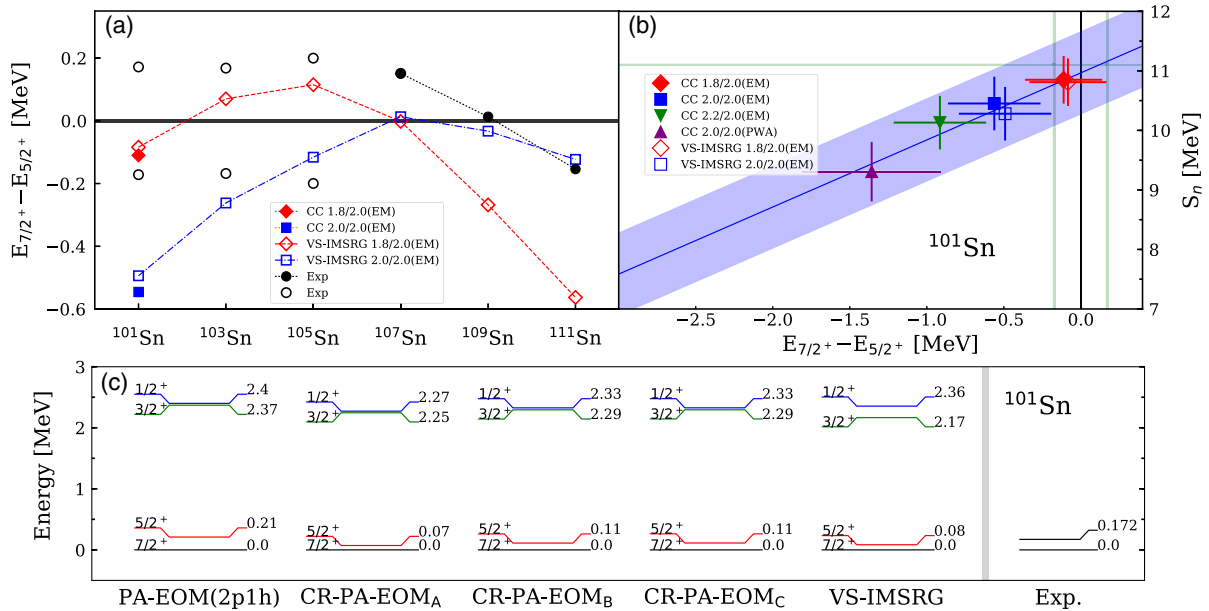


FIG. 3. Panel (a) shows the energy splitting between the lowest  $J^\pi = 7/2^+$  and  $5/2^+$  states in light odd-mass tin isotopes. Data are black circles for isotopes with definite (full) and tentative spin assignments (open symbols). Theoretical results are from coupled cluster (full) and VS-IMSRG (open symbols) for the interactions as indicated. Panel (b) shows the correlation between the neutron separation energy  $S_n$  and the energy splitting between the lowest  $J^\pi = 7/2^+$  and  $5/2^+$  states for the interactions and computational method as labeled (symbols with error bars and an encompassing blue uncertainty band) compared to data (vertical and horizontal green lines). Panel (c) shows the low-lying levels in  $^{101}\text{Sn}$  based on the chiral interaction 1.8/2.0(EM) computed with various coupled-cluster equation-of-motion (EOM) methods, the VS-IMSRG, and compared to data.

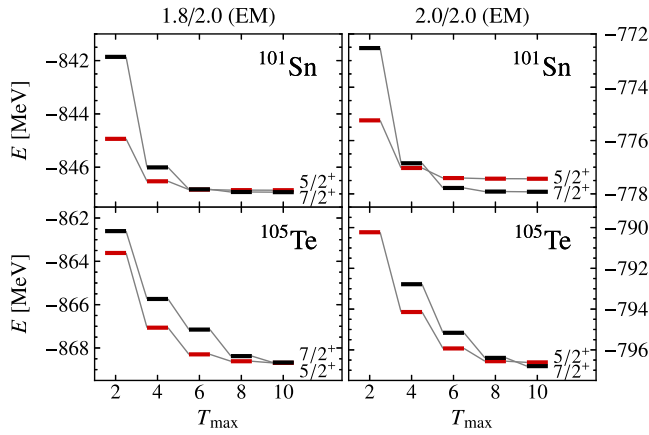


FIG. 4. Ground and first excited states in  $^{101}\text{Sn}$  and  $^{105}\text{Te}$  obtained in VS-IMSRG for the 1.8/2.0(EM) and 2.0/2.0(EM) interactions, with spins  $J^\pi = 5/2^+$  (red) and  $J^\pi = 7/2^+$  (black).

fine details can be unambiguously resolved will require more work.

Figure 4 shows the convergence of the  $5/2^+$  and  $7/2^+$  states in  $^{101}\text{Sn}$  and  $^{105}\text{Te}$  with the number of particle-hole excitations ( $T_{\text{max}}$ ) in the importance-truncated large-scale shell-model calculations using the 1.8/2.0(EM) and 2.0/2.0(EM) interactions. In both,  $^{101}\text{Sn}$  and  $^{105}\text{Te}$ , we obtain nearly degenerate  $J^\pi = 5/2^+$  and  $7/2^+$  states consistent with data.

*Conclusions and outlook.*—Our computations demonstrated that tin nuclei can be described by  $NN$  and  $NNN$  interactions constrained by few-body data. We found that  $^{100}\text{Sn}$  is doubly magic and presented results and predictions for its structure and low-lying collectivity. For an increased precision of excited states in  $^{101}\text{Sn}$ , we developed a method that includes three-particle–two-hole excitations in our coupled-cluster calculations. Systematic uncertainties from the employed interactions are significant. One interaction reproduced both binding energies and the near degeneracy between the lowest  $J^\pi = 5/2^+$  and  $7/2^+$  states in the odd-mass isotopes  $^{101-111}\text{Sn}$  and  $^{105}\text{Te}$ . A more systematic approach to nuclear interactions, including all contributions to a given order, as well as one based on new developments such as Refs. [83,84] or the inclusion of delta degrees of freedom [85,86], may be required to reduce systematic uncertainties.

We thank K. Hebeler for providing us with matrix elements in Jacobi coordinates for the  $NNN$  interaction at next-to-next-to-leading order. This work was supported by the Office of Nuclear Physics, U.S. Department of Energy, under Grants No. DE-FG02-96ER40963, No. DE-SC0008499, and No. DE-SC0018223 (NUCLEI SciDAC Collaboration), by Field Work Proposal No. ERKBP57 at Oak Ridge National Laboratory (ORNL), by ERC Grant No. 307986 STRONGINT, by the BMBF under Contract No. 05P15RDFN1, by the DFG under Grant No. SFB 1245 DFG, by the National Research Council Canada, and by

NSERC. Computer time was provided by the Innovative and Novel Computational Impact on Theory and Experiment (INCITE) program. This research used resources of the Oak Ridge Leadership Computing Facility located at ORNL, which is supported by the Office of Science of the Department of Energy under Contract No. DE-AC05-00OR22725. Computations were also performed at the LICHTENBERG high-performance computer of the TU Darmstadt, the Jülich Supercomputing Center (JURECA), the LOEWE-CSC Frankfurt, and at the Max-Planck-Institute for Nuclear Physics.

This manuscript has been authored by UT-Battelle, LLC under Contract No. DE-AC05-00OR22725 with the U.S. Department of Energy. The United States government retains, and the publisher, by accepting the article for publication, acknowledges that the United States government retains, a nonexclusive, paid-up, irrevocable, worldwide license to publish or reproduce the published form of this manuscript, or allow others to do so, for United States government purposes. The Department of Energy will provide public access to these results of federally sponsored research in accordance with the DOE Public Access Plan.

- [1] M. Lewitowicz, R. Anne, G. Auger, D. Bazin, C. Borcea, V. Borrel, J. M. Corre, T. Dörfner, A. Fomichov, R. Grzywacz, D. Guillemaud-Mueller, R. Hue, M. Huyse, Z. Janas, H. Keller, S. Lukyanov, A. C. Mueller, Yu. Penionzhkevich, M. Pfützner, F. Pougheon *et al.*, Identification of the doubly magic nucleus  $^{100}\text{Sn}$  in the reaction  $^{112}\text{Sn} + ^{\text{nat}}\text{Ni}$  at 63 MeV/nucleon, *Phys. Lett. B* **332**, 20 (1994).
- [2] C. B. Hinke, M. Böhmer, P. Boutachkov, T. Faestermann, H. Geissel, J. Gerl, R. Gernhäuser, M. Gorska, A. Gottardo, H. Grawe, J. L. Grebosz, R. Krücken, N. Kurz, Z. Liu, L. Maier, F. Nowacki, S. Pietri, Zs. Podolyák, K. Sieja, K. Steiger *et al.*, Superallowed Gamow-Teller decay of the doubly magic nucleus  $^{100}\text{Sn}$ , *Nature (London)* **486**, 341 (2012).
- [3] J. Erler, N. Birge, M. Kortelainen, W. Nazarewicz, E. Olsen, A. M. Perhac, and M. Stoitsov, The limits of the nuclear landscape, *Nature (London)* **486**, 509 (2012).
- [4] S. N. Liddick, R. Grzywacz, C. Mazzocchi, R. D. Page, K. P. Rykaczewski, J. C. Batchelder, C. R. Bingham, I. G. Darby, G. Drafta, C. Goodin, C. J. Gross, J. H. Hamilton, A. A. Hecht, J. K. Hwang, S. Ilyushkin, D. T. Joss, A. Korgul, W. Królas, K. Lagergren, K. Li, M. N. Tantawy, J. Thomson, and J. A. Winger, Discovery of  $^{109}\text{Xe}$  and  $^{105}\text{Te}$ : Superallowed  $\alpha$  Decay near Doubly Magic  $^{100}\text{Sn}$ , *Phys. Rev. Lett.* **97**, 082501 (2006).
- [5] D. Seweryniak, K. Starosta, C. N. Davids, S. Gros, A. A. Hecht, N. Hotelling, T. L. Khoo, K. Lagergren, G. Lotay, D. Peterson, A. Robinson, C. Vaman, W. B. Walters, P. J. Woods, and S. Zhu,  $\alpha$  decay of  $^{105}\text{Te}$ , *Phys. Rev. C* **73**, 061301 (2006).
- [6] T. Faestermann, M. Górska, and H. Grawe, The structure of  $^{100}\text{Sn}$  and neighbouring nuclei, *Prog. Part. Nucl. Phys.* **69**, 85 (2013).

- [7] D. Seweryniak, M. P. Carpenter, S. Gros, A. A. Hecht, N. Hoteling, R. V. F. Janssens, T. L. Khoo, T. Lauritsen, C. J. Lister, G. Lotay, D. Peterson, A. P. Robinson, W. B. Walters, X. Wang, P. J. Woods, and S. Zhu, Single-Neutron States in  $^{101}\text{Sn}$ , *Phys. Rev. Lett.* **99**, 022504 (2007).
- [8] I. G. Darby, R. K. Grzywacz, J. C. Batchelder, C. R. Bingham, L. Cartegni, C. J. Gross, M. Hjorth-Jensen, D. T. Joss, S. N. Liddick, W. Nazarewicz, S. Padgett, R. D. Page, T. Papenbrock, M. M. Rajabali, J. Rotureau, and K. P. Rykaczewski, Orbital Dependent Nucleonic Pairing in the Lightest Known Isotopes of Tin, *Phys. Rev. Lett.* **105**, 162502 (2010).
- [9] A. Banu, J. Gerl, C. Fahlander, M. Górska, H. Grawe, T. R. Saito, H.-J. Wollersheim, E. Caurier, T. Engeland, A. Gniady, M. Hjorth-Jensen, F. Nowacki, T. Beck, F. Becker, P. Bednarczyk, M. A. Bentley, A. Bürger, F. Cristancho, G. de Angelis, Zs. Dombrádi *et al.*,  $^{108}\text{Sn}$  studied with intermediate-energy Coulomb excitation, *Phys. Rev. C* **72**, 061305 (2005).
- [10] C. Vaman, C. Andreoiu, D. Bazin, A. Becerril, B. A. Brown, C. M. Campbell, A. Chester, J. M. Cook, D. C. Dinca, A. Gade, D. Galaviz, T. Glasmacher, M. Hjorth-Jensen, M. Horoi, D. Miller, V. Moeller, W. F. Mueller, A. Schiller, K. Starosta, A. Stolz *et al.*,  $Z = 50$  Shell Gap near  $^{100}\text{Sn}$  from Intermediate-Energy Coulomb Excitations in Even-Mass  $^{106-112}\text{Sn}$  Isotopes, *Phys. Rev. Lett.* **99**, 162501 (2007).
- [11] A. Ekström, J. Cederkäll, C. Fahlander, M. Hjorth-Jensen, F. Ames, P. A. Butler, T. Davinson, J. Eberth, F. Fincke, A. Górgen, M. Górska, D. Habs, A. M. Hurst, M. Huyse, O. Ivanov, J. Iwanicki, O. Kester, U. Köster, B. A. Marsh, J. Mierzejewski *et al.*,  $0_{gs}^+ \rightarrow 2_1^+$  Transition Strengths in  $^{106}\text{Sn}$  and  $^{108}\text{Sn}$ , *Phys. Rev. Lett.* **101**, 012502 (2008).
- [12] G. Guastalla, D. D. DiJulio, M. Górska, J. Cederkäll, P. Boutachkov, P. Golubev, S. Pietri, H. Grawe, F. Nowacki, K. Sieja, A. Algora, F. Ameil, T. Arici, A. Atac, M. A. Bentley, A. Blazhev, D. Bloor, S. Brambilla, N. Braun, F. Camera *et al.*, Coulomb Excitation of  $^{104}\text{Sn}$  and the Strength of the  $^{100}\text{Sn}$  Shell Closure, *Phys. Rev. Lett.* **110**, 172501 (2013).
- [13] V. M. Bader, A. Gade, D. Weisshaar, B. A. Brown, T. Baugher, D. Bazin, J. S. Berryman, A. Ekström, M. Hjorth-Jensen, S. R. Stroberg, W. B. Walters, K. Wimmer, and R. Winkler, Quadrupole collectivity in neutron-deficient Sn nuclei:  $^{104}\text{Sn}$  and the role of proton excitations, *Phys. Rev. C* **88**, 051301 (2013).
- [14] P. Doornenbal, S. Takeuchi, N. Aoi, M. Matsushita, A. Obertelli, D. Steppenbeck, H. Wang, L. Audirac, H. Baba, P. Bednarczyk, S. Boissinot, M. Ciemala, A. Corsi, T. Furumoto, T. Isobe, A. Jungclaus, V. Lapoux, J. Lee, K. Matsui, T. Motobayashi *et al.*, Intermediate-energy Coulomb excitation of  $^{104}\text{Sn}$ : Moderate  $E2$  strength decrease approaching  $^{100}\text{Sn}$ , *Phys. Rev. C* **90**, 061302 (2014).
- [15] A. Jungclaus *et al.*, Evidence for reduced collectivity around the neutron mid-shell in the stable even-mass Sn isotopes from new lifetime measurements, *Phys. Lett. B* **695**, 110 (2011).
- [16] J. M. Allmond, D. C. Radford, C. Baktash, J. C. Batchelder, A. Galindo-Uribarri, C. J. Gross, P. A. Hausladen, K. Lagergren, Y. Laroche, E. Padilla-Rodal, and C.-H. Yu, Coulomb excitation of  $^{124,126,128}\text{Sn}$ , *Phys. Rev. C* **84**, 061303 (2011).
- [17] J. M. Allmond *et al.*, Double-Magic Nature of  $^{132}\text{Sn}$  and  $^{208}\text{Pb}$  through Lifetime and Cross-Section Measurements, *Phys. Rev. Lett.* **112**, 172701 (2014).
- [18] J. M. Allmond, A. E. Stuchbery, A. Galindo-Uribarri, E. Padilla-Rodal, D. C. Radford, J. C. Batchelder, C. R. Bingham, M. E. Howard, J. F. Liang, B. Manning, S. D. Pain, N. J. Stone, R. L. Varner, and C.-H. Yu, Investigation into the semimagic nature of the tin isotopes through electromagnetic moments, *Phys. Rev. C* **92**, 041303 (2015).
- [19] M. Lipoglavšek, C. Baktash, J. Blomqvist, M. P. Carpenter, D. J. Dean, T. Engeland, C. Fahlander, M. Hjorth-Jensen, R. V. F. Janssens, A. Likar, J. Nyberg, E. Osnes, S. D. Paul, A. Piechaczek, D. C. Radford, D. Rudolph, D. Seweryniak, D. G. Sarantites, M. Vencelj, and C.-H. Yu, Breakup of the doubly magic  $^{100}\text{Sn}$  core, *Phys. Rev. C* **66**, 011302 (2002).
- [20] A. Blazhev, M. Górska, H. Grawe, J. Nyberg, M. Palacz, E. Caurier, O. Dorvaux, A. Gadea, F. Nowacki, C. Andreoiu, G. de Angelis, D. Balabanski, Ch. Beck, B. Cederwall, D. Curien, J. Döring, J. Ekman, C. Fahlander, K. Lagergren, J. Ljungvall *et al.*, Observation of a core-excited  $E4$  isomer in  $^{98}\text{Cd}$ , *Phys. Rev. C* **69**, 064304 (2004).
- [21] P. Boutachkov, M. Górska, H. Grawe, A. Blazhev, N. Braun, T. S. Brock, Z. Liu, B. S. Nara Singh, R. Wadsworth, S. Pietri, C. Domingo-Pardo, I. Kojouharov, L. Cáceres, T. Engert, F. Farinon, J. Gerl, N. Goel, J. Grbosz, R. Hoischen, N. Kurz *et al.*, High-spin isomers in  $^{96}\text{Ag}$ : Excitations across the  $Z = 38$  and  $Z = 50$ ,  $N = 50$  closed shells, *Phys. Rev. C* **84**, 044311 (2011).
- [22] T. S. Brock, B. S. Nara Singh, P. Boutachkov, N. Braun, A. Blazhev, Z. Liu, R. Wadsworth, M. Górska, H. Grawe, S. Pietri, C. Domingo-Pardo, D. Rudolph, S. J. Steer, A. Ataç, L. Bettermann, L. Cáceres, T. Engert, K. Eppinger, T. Faestermann, F. Farinon *et al.* (RISING Collaboration), Observation of a new high-spin isomer in  $^{94}\text{Pd}$ , *Phys. Rev. C* **82**, 061309 (2010).
- [23] E. Caurier, F. Nowacki, A. Poves, and K. Sieja, Collectivity in the light xenon isotopes: A shell model study, *Phys. Rev. C* **82**, 064304 (2010).
- [24] M. Hjorth-Jensen, T. T. S. Kuo, and E. Osnes, Realistic effective interactions for nuclear systems, *Phys. Rep.* **261**, 125 (1995).
- [25] U. Van Kolck, Effective field theory of nuclear forces, *Prog. Part. Nucl. Phys.* **43**, 337 (1999).
- [26] E. Epelbaum, H.-W. Hammer, and U.-G. Meißner, Modern theory of nuclear forces, *Rev. Mod. Phys.* **81**, 1773 (2009).
- [27] R. Machleidt and D. R. Entem, Chiral effective field theory and nuclear forces, *Phys. Rep.* **503**, 1 (2011).
- [28] P. Navrátil, S. Quaglioni, I. Stetcu, and B. R. Barrett, Recent developments in no-core shell-model calculations, *J. Phys. G* **36**, 083101 (2009).
- [29] B. R. Barrett, P. Navrátil, and J. P. Vary, *Ab initio* no core shell model, *Prog. Part. Nucl. Phys.* **69**, 131 (2013).
- [30] G. Hagen, T. Papenbrock, M. Hjorth-Jensen, and D. J. Dean, Coupled-cluster computations of atomic nuclei, *Rep. Prog. Phys.* **77**, 096302 (2014).
- [31] H. Hergert, S. K. Bogner, T. D. Morris, A. Schwenk, and K. Tsukiyama, The in-medium similarity renormalization

- group: A novel *ab initio* method for nuclei, *Phys. Rep.* **621**, 165 (2016).
- [32] S. C. Pieper and R. B. Wiringa, Quantum Monte Carlo calculations of light nuclei, *Annu. Rev. Nucl. Part. Sci.* **51**, 53 (2001).
- [33] B. Mihaila and J. H. Heisenberg, Microscopic Calculation of the Inclusive Electron Scattering Structure Function in  $^{16}\text{O}$ , *Phys. Rev. Lett.* **84**, 1403 (2000).
- [34] D. J. Dean and M. Hjorth-Jensen, Coupled-cluster approach to nuclear physics, *Phys. Rev. C* **69**, 054320 (2004).
- [35] W. H. Dickhoff and C. Barbieri, Self-consistent Green's function method for nuclei and nuclear matter, *Prog. Part. Nucl. Phys.* **52**, 377 (2004).
- [36] G. Hagen, T. Papenbrock, D. J. Dean, and M. Hjorth-Jensen, Medium-Mass Nuclei from Chiral Nucleon-Nucleon Interactions, *Phys. Rev. Lett.* **101**, 092502 (2008).
- [37] G. Hagen, T. Papenbrock, D. J. Dean, and M. Hjorth-Jensen, *Ab initio* coupled-cluster approach to nuclear structure with modern nucleon-nucleon interactions, *Phys. Rev. C* **82**, 034330 (2010).
- [38] K. Tsukiyama, S. K. Bogner, and A. Schwenk, In-Medium Similarity Renormalization Group For Nuclei, *Phys. Rev. Lett.* **106**, 222502 (2011).
- [39] R. Roth, S. Binder, K. Vobig, A. Calci, J. Langhammer, and P. Navrátil, Medium-Mass Nuclei with Normal-Ordered Chiral  $NN+3N$  Interactions, *Phys. Rev. Lett.* **109**, 052501 (2012).
- [40] H. Hergert, S. K. Bogner, S. Binder, A. Calci, J. Langhammer, R. Roth, and A. Schwenk, In-medium similarity renormalization group with chiral two- plus three-nucleon interactions, *Phys. Rev. C* **87**, 034307 (2013).
- [41] V. Somà, A. Cipollone, C. Barbieri, P. Navrátil, and T. Duguet, Chiral two- and three-nucleon forces along medium-mass isotope chains, *Phys. Rev. C* **89**, 061301 (2014).
- [42] S. Binder, P. Piecuch, A. Calci, J. Langhammer, P. Navrátil, and R. Roth, Extension of coupled-cluster theory with a noniterative treatment of connected triply excited clusters to three-body Hamiltonians, *Phys. Rev. C* **88**, 054319 (2013).
- [43] T. A. Lähde, E. Epelbaum, H. Krebs, D. Lee, U.-G. Meißner, and G. Rupak, Lattice effective field theory for medium-mass nuclei, *Phys. Lett. B* **732**, 110 (2014).
- [44] S. Binder, J. Langhammer, A. Calci, and R. Roth, *Ab initio* path to heavy nuclei, *Phys. Lett. B* **736**, 119 (2014).
- [45] K. Hebeler, S. K. Bogner, R. J. Furnstahl, A. Nogga, and A. Schwenk, Improved nuclear matter calculations from chiral low-momentum interactions, *Phys. Rev. C* **83**, 031301 (2011).
- [46] A. Ekström, G. Baardsen, C. Forssén, G. Hagen, M. Hjorth-Jensen, G. R. Jansen, R. Machleidt, W. Nazarewicz, T. Papenbrock, J. Sarich, and S. M. Wild, Optimized Chiral Nucleon-Nucleon Interaction at Next-to-Next-to-Leading Order, *Phys. Rev. Lett.* **110**, 192502 (2013).
- [47] A. Ekström, G. R. Jansen, K. A. Wendt, G. Hagen, T. Papenbrock, B. D. Carlsson, C. Forssén, M. Hjorth-Jensen, P. Navrátil, and W. Nazarewicz, Accurate nuclear radii and binding energies from a chiral interaction, *Phys. Rev. C* **91**, 051301 (2015).
- [48] A. Ekström, G. Hagen, T. D. Morris, T. Papenbrock, and P. D. Schwartz, Delta isobars and nuclear saturation, *Phys. Rev. C* **97**, 024332 (2018).
- [49] G. Hagen, A. Ekström, C. Forssén, G. R. Jansen, W. Nazarewicz, T. Papenbrock, K. A. Wendt, S. Bacca, N. Barnea, B. Carlsson, C. Drischler, K. Hebeler, M. Hjorth-Jensen, M. Miorelli, G. Orlandini, A. Schwenk, and J. Simonis, Neutron and weak-charge distributions of the  $^{48}\text{Ca}$  nucleus, *Nat. Phys.* **12**, 186 (2016).
- [50] G. Hagen, M. Hjorth-Jensen, G. R. Jansen, and T. Papenbrock, Emergent properties of nuclei from *ab initio* coupled-cluster calculations, *Phys. Scr.* **91**, 063006 (2016).
- [51] G. Hagen, G. R. Jansen, and T. Papenbrock, Structure of  $^{78}\text{Ni}$  from First-Principles Computations, *Phys. Rev. Lett.* **117**, 172501 (2016).
- [52] J. Simonis, K. Hebeler, J. D. Holt, J. Menendez, and A. Schwenk, Exploring *sd*-shell nuclei from two- and three-nucleon interactions with realistic saturation properties, *Phys. Rev. C* **93**, 011302 (2016).
- [53] R. F. Garcia Ruiz, M. L. Bissell, K. Blaum, A. Ekström, N. Frömmgen, G. Hagen, M. Hammen, K. Hebeler, J. D. Holt, G. R. Jansen, M. Kowalska, K. Kreim, W. Nazarewicz, R. Neugart, G. Neyens, W. Nörtershäuser, T. Papenbrock, J. Papuga, A. Schwenk, J. Simonis *et al.*, Unexpectedly large charge radii of neutron-rich calcium isotopes, *Nat. Phys.* **12**, 594 (2016).
- [54] J. Simonis, S. R. Stroberg, K. Hebeler, J. D. Holt, and A. Schwenk, Saturation with chiral interactions and consequences for finite nuclei, *Phys. Rev. C* **96**, 014303 (2017).
- [55] R. J. Bartlett and M. Musiał, Coupled-cluster theory in quantum chemistry, *Rev. Mod. Phys.* **79**, 291 (2007).
- [56] S. R. Stroberg, A. Calci, H. Hergert, J. D. Holt, S. K. Bogner, R. Roth, and A. Schwenk, Nucleus-Dependent Valence-Space Approach to Nuclear Structure, *Phys. Rev. Lett.* **118**, 032502 (2017).
- [57] C. Stumpf, J. Braun, and R. Roth, Importance-truncated large-scale shell model, *Phys. Rev. C* **93**, 021301 (2016).
- [58] S. K. Bogner, R. J. Furnstahl, and R. J. Perry, Similarity renormalization group for nucleon-nucleon interactions, *Phys. Rev. C* **75**, 061001 (2007).
- [59] D. R. Entem and R. Machleidt, Accurate charge-dependent nucleon-nucleon potential at fourth order of chiral perturbation theory, *Phys. Rev. C* **68**, 041001 (2003).
- [60] U. van Kolck, Few-nucleon forces from chiral Lagrangians, *Phys. Rev. C* **49**, 2932 (1994).
- [61] E. Epelbaum, A. Nogga, W. Glöckle, H. Kamada, U.-G. Meißner, and H. Witała, Three-nucleon forces from chiral effective field theory, *Phys. Rev. C* **66**, 064001 (2002).
- [62] K. Hebeler, H. Krebs, E. Epelbaum, J. Golak, and R. Skibiński, Efficient calculation of chiral three-nucleon forces up to  $N^3\text{LO}$  for *ab initio* studies, *Phys. Rev. C* **91**, 044001 (2015).
- [63] A. Nogga, S. K. Bogner, and A. Schwenk, Low-momentum interaction in few-nucleon systems, *Phys. Rev. C* **70**, 061002 (2004).
- [64] G. Hagen, T. Papenbrock, D. J. Dean, A. Schwenk, A. Nogga, M. Włoch, and P. Piecuch, Coupled-cluster theory for three-body Hamiltonians, *Phys. Rev. C* **76**, 034302 (2007).
- [65] H. Kümmel, K. H. Lührmann, and J. G. Zabolitzky, Many-fermion theory in exp *S*- (or coupled cluster) form, *Phys. Rep.* **36**, 1 (1978).

- [66] M. Włoch, D. J. Dean, J. R. Gour, M. Hjorth-Jensen, K. Kowalski, T. Papenbrock, and P. Piecuch, *Ab Initio* Coupled-Cluster Study of  $^{16}\text{O}$ , *Phys. Rev. Lett.* **94**, 212501 (2005).
- [67] R. Roth, J. Langhammer, A. Calci, S. Binder, and P. Navrátil, Similarity-Transformed Chiral  $NN + 3N$  Interactions for the *Ab Initio* Description of  $^{12}\text{C}$  and  $^{16}\text{O}$ , *Phys. Rev. Lett.* **107**, 072501 (2011).
- [68] A. G. Taube and R. J. Bartlett, Improving upon CCSD(T): Lambda CCSD(T): I. Potential energy surfaces, *J. Chem. Phys.* **128**, 044110 (2008).
- [69] J. D. Watts and R. J. Bartlett, Economical triple excitation equation-of-motion coupled-cluster methods for excitation energies, *Chem. Phys. Lett.* **233**, 81 (1995).
- [70] J. R. Gour, P. Piecuch, and M. Włoch, Active-space equation-of-motion coupled-cluster methods for excited states of radicals and other open-shell systems: EA-EOMCCSDt and IP-EOMCCSDt, *J. Chem. Phys.* **123**, 134113 (2005).
- [71] G. R. Jansen, M. Hjorth-Jensen, G. Hagen, and T. Papenbrock, Toward open-shell nuclei with coupled-cluster theory, *Phys. Rev. C* **83**, 054306 (2011).
- [72] G. R. Jansen, Spherical coupled-cluster theory for open-shell nuclei, *Phys. Rev. C* **88**, 024305 (2013).
- [73] K. Kowalski and P. Piecuch, The method of moments of coupled-cluster equations and the renormalized CCSD[T], CCSD(T), CCSD(TQ), and CCSDT(Q) approaches, *J. Chem. Phys.* **113**, 18 (2000).
- [74] P. Piecuch, K. Kowalski, I. S. O. Pimienta, and M. J. McGuire, Recent advances in electronic structure theory: Method of moments of coupled-cluster equations and renormalized coupled-cluster approaches, *Int. Rev. Phys. Chem.* **21**, 527 (2002).
- [75] K. Kowalski, D. J. Dean, M. Hjorth-Jensen, T. Papenbrock, and P. Piecuch, Coupled Cluster Calculations of Ground and Excited States of Nuclei, *Phys. Rev. Lett.* **92**, 132501 (2004).
- [76] K. Tsukiyama, S. K. Bogner, and A. Schwenk, In-medium similarity renormalization group for open-shell nuclei, *Phys. Rev. C* **85**, 061304 (2012).
- [77] S. K. Bogner, H. Hergert, J. D. Holt, A. Schwenk, S. Binder, A. Calci, J. Langhammer, and R. Roth, Nonperturbative Shell-Model Interactions from the in-Medium Similarity Renormalization Group, *Phys. Rev. Lett.* **113**, 142501 (2014).
- [78] S. R. Stroberg, H. Hergert, J. D. Holt, S. K. Bogner, and A. Schwenk, Ground and excited states of doubly open-shell nuclei from *ab initio* valence-space Hamiltonians, *Phys. Rev. C* **93**, 051301 (2016).
- [79] T. Björnstad, L.-E. De Geer, G. T. Ewan, P. G. Hansen, B. Jonson, K. Kawade, A. Kerek, W.-D. Lauppe, H. Lawin, S. Mattsson, and K. Sistemich, Structure of the levels in the doubly magic nucleus  $^{132}\text{Sn}_{82}$ , *Phys. Lett.* **91B**, 35 (1980).
- [80] K. L. Jones, A. S. Adekola, D. W. Bardayan, J. C. Blackmon, K. Y. Chae, K. A. Chipps, J. A. Cizewski, L. Erikson, C. Harlin, R. Hatarik, R. Kapler, R. L. Kozub, J. F. Liang, R. Livesay, Z. Ma, B. H. Moazen, C. D. Nesaraja, F. M. Nunes, S. D. Pain, N. P. Patterson *et al.*, The magic nature of  $^{132}\text{Sn}$  explored through the single-particle states of  $^{133}\text{Sn}$ , *Nature (London)* **465**, 454 (2010).
- [81] G. Cerizza, A. Ayres, K. L. Jones, R. Grzywacz, A. Bey, C. Bingham, L. Cartegni, D. Miller, S. Padgett, T. Baugher, D. Bazin, J. S. Berryman, A. Gade, S. McDaniel, A. Ratkiewicz, A. Shore, S. R. Stroberg, D. Weisshaar, K. Wimmer, R. Winkler *et al.*, Structure of  $^{107}\text{Sn}$  studied through single-neutron knockout reactions, *Phys. Rev. C* **93**, 021601 (2016).
- [82] R. F. Garcia Ruiz *et al.*, IS613: Laser spectroscopy of neutron-deficient Sn isotopes,” CERN Proposal No. INTC-P-456 CERN-INTC-2016-006, 2016.
- [83] J. A. Melendez, S. Wesolowski, and R. J. Furnstahl, Bayesian truncation errors in chiral effective field theory: Nucleon-nucleon observables, *Phys. Rev. C* **96**, 024003 (2017).
- [84] P. Reinert, H. Krebs, and E. Epelbaum, Semilocal momentum-space regularized chiral two-nucleon potentials up to fifth order, *arXiv:1711.08821*.
- [85] A. Ekström, G. Hagen, T. D. Morris, T. Papenbrock, and P. D. Schwartz,  $\Delta$  isobars and nuclear saturation, *Phys. Rev. C* **97**, 024332 (2018).
- [86] M. Piarulli, A. Baroni, L. Girlanda, A. Kievsky, A. Lovato, Ewing Lusk, L. E. Marcucci, S. C. Pieper, R. Schiavilla, M. Viviani, and R. B. Wiringa, Light-Nuclei Spectra from Chiral Dynamics, *Phys. Rev. Lett.* **120**, 052503 (2018).